10.1098/rsta.2000.0811

THE ROYAL SOCIETY

Interfacial properties of model colloid–polymer mixtures

BY R. EVANS[1], J. M. BRADER[1], R. ROTH[1], M. DIJKSTRA[2], M. SCHMIDT[3] AND H. LÖWEN[3]

[1]*H. H. Wills Physics Laboratory, University of Bristol, Bristol BS8 1TL, UK*
[2]*Debye Institute, Soft Condensed Matter Physics, Utrecht University, Princetonplein 5, 3584 CC Utrecht, The Netherlands*
[3]*Institut für Theoretische Physik II, Universität Düsseldorf, Universitätsstrasse 1, D-40225 Düsseldorf, Germany*

We summarize the main results of our recent investigations of the interfacial properties of the simplest model of a colloid–polymer mixture, namely that introduced by Asakura & Oosawa and by Vrij, in which colloid–colloid and colloid–polymer interactions are treated as hard sphere-like, while the polymer–polymer interaction is ideal (perfectly interpenetrating coils). In spite of its simplicity, we find that the model exhibits rich interfacial behaviour which depends on the size ratio $q \equiv \sigma_p/\sigma_c$, where σ_p and σ_c denote the diameters of polymer and colloid, respectively. For highly asymmetric mixtures, $q < 0.1547$, an explicit and exact mapping of the binary mixture to an effective one-component Hamiltonian for the colloids allows one to perform computer simulations for inhomogeneous mixtures. We investigate a mixture with $q = 0.1$ and find that small amounts of polymer give rise to strong depletion effects at a hard wall. The colloid density at contact with the wall is several times greater than that for pure hard spheres at a hard wall. However, for states removed from the bulk fluid–solid coexistence curve we find no evidence of wall-induced crystallization. In order to treat less asymmetric cases, where stable fluid–fluid demixing occurs in bulk, we have designed a density functional theory specifically for this model mixture. For $q = 0.6$ we find a first order wetting transition from partial to complete wetting by the colloid-rich phase at the hard-wall–colloid-poor interface as the packing fraction η_p^r of polymer in the reservoir is decreased. At a slightly higher value of η_p^r, there is a novel *single* layering transition, characterized by a jump in the densities in the first two adsorbed layers, as the bulk colloid packing fraction η_c is increased. The same density functional has been used to investigate the surface tension and colloid and polymer density profiles at the free interface between the demixed fluid phases.

Keywords: colloid–polymer mixtures; depletion forces; effective Hamiltonians; wetting and layering transitions; surface tension; adsorption

1. Introduction

It is well known that the addition of non-adsorbing polymers to a colloidal suspension gives rise to an attractive interaction between the colloidal particles. The physical mechanism for this phenomenon is the depletion effect, i.e. an effective attractive interaction is induced by the exclusion of polymer from a depletion zone

between colloids; the range of the interaction is set by the diameter of the polymer coils and the strength of the attraction is determined by the chemical potential of the polymer reservoir (Asakura & Oosawa 1954). The simplest model of the binary colloid–polymer mixture treats the colloids as hard spheres, with diameter σ_c, and the polymers as ideal interpenetrating coils, as regards their mutual interactions. It requires the polymers to be excluded by a centre of mass distance $(\sigma_c + \sigma_p)/2$ from the colloids (Asakura & Oosawa 1954; Vrij 1976). The parameter σ_p is usually taken to be $2R_g$, where R_g is the radius of gyration of the polymer. Assuming that the polymer is ideal is a drastic oversimplification. It is a situation achieved (approximately) for dilute solutions of polymer in a theta solvent. Nevertheless, this binary Asakura–Oosawa (AO) model does capture the main features of the observed variation of the bulk phase behaviour of real colloid–polymer mixtures with increasing size ratio $q = \sigma_p/\sigma_c$ (Gast *et al.* 1983; Lekkerkerker *et al.* 1992; Ilett *et al.* 1995). Surprisingly, little attention has been paid to *inhomogeneous* colloid–polymer mixtures where the average density profiles of both species are spatially varying. Such situations arise in adsorption at a solid substrate, in mixtures confined in narrow pores, at the planar interface between two coexisting (colloid-rich and polymer-rich) fluid phases and in colloidal crystals. Given the usefulness of the AO model for bulk phase behaviour, where it predicts stable solid, liquid and gas colloid phases for sufficiently large q, it is natural to investigate its properties for interfaces. Such a strategy is common in statistical physics. The Ising or lattice gas model provides only a crude description of a real liquid–gas (bulk condensation) phase transition but yields a wealth of predictions for surface transitions, with the substrate modelled as a simple external field, most of which have been found in adsorption experiments. Here we show that the interfacial properties of the AO model should be richer than those of the bulk and argue that adsorption-type experiments on real colloid–polymer mixtures could reveal striking phenomena. The results which emerge from the AO model are interesting from a fundamental statistical mechanics viewpoint since the *bare* interactions between the constituent particles are either hard or ideal; surface and bulk transitions are purely entropically driven. *Depletion* effects give rise to effective attractive interactions between colloidal particles or between colloids and a hard wall.

This paper describes the two different strategies we have employed in tackling the statistical mechanics of the AO model. The first involves integrating out the polymer degrees of freedom to obtain an effective one-component Hamiltonian for the colloids, while the second is based on a new density functional theory specifically designed for the binary AO mixture.

2. Bare and effective Hamitonians

We consider an extreme non-additive binary hard sphere mixture consisting of N_c hard spheres, representing colloid, and N_p interpenetrable, non-interacting particles, representing ideal polymer, in a volume V at temperature T. This is a reasonable model of a colloid–polymer mixture, as the interaction between sterically stabilized colloidal particles can be made close to that of hard spheres, and dilute solutions of polymer in a theta solvent are very weakly interacting. We implicitly assume that any solvent molecules which are present in a real suspension can be treated as an inert continuum, and thus have no effect on bulk or interfacial properties. The colloids interact via the hard sphere potential, with diameter σ_c, and the polymers

are excluded from the colloids to a centre of mass distance $(\sigma_c + \sigma_p)/2$. This simple model of an idealized colloid–polymer mixture is often called the Asakura–Oosawa (AO) model although it was first defined explicitly by Vrij (1976). It is specified by the bare pair potentials:

$$\left.\begin{aligned} \phi_{cc}(R_{ij}) &= \begin{cases} \infty & \text{for } R_{ij} < \sigma_c, \\ 0 & \text{otherwise}, \end{cases} \\ \phi_{cp}(|\boldsymbol{R}_i - \boldsymbol{r}_j|) &= \begin{cases} \infty & \text{for } |\boldsymbol{R}_i - \boldsymbol{r}_j| < \frac{1}{2}(\sigma_c + \sigma_p), \\ 0 & \text{otherwise}, \end{cases} \\ \phi_{pp}(r_{ij}) &= 0, \end{aligned}\right\} \tag{2.1}$$

where $\boldsymbol{R}$ and $\boldsymbol{r}$ denote colloid and polymer centre of mass coordinates, respectively, with $R_{ij} = |\boldsymbol{R}_i - \boldsymbol{R}_j|$ and $r_{ij} = |\boldsymbol{r}_i - \boldsymbol{r}_j|$. The Hamiltonian thus consists of (trivial) kinetic energy contributions and a sum of interaction terms: $H = H_{cc} + H_{cp} + H_{pp}$, where

$$\left.\begin{aligned} H_{cc} &= \sum_{i<j}^{N_c} \phi_{cc}(R_{ij}), \\ H_{cp} &= \sum_{i}^{N_c} \sum_{j}^{N_p} \phi_{cp}(|\boldsymbol{R}_i - \boldsymbol{r}_j|), \\ H_{pp} &= \sum_{i<j}^{N_p} \phi_{pp}(R_{ij}) = 0. \end{aligned}\right\} \tag{2.2}$$

Following the treatment of the bulk (Dijkstra *et al.* 1999*a*, *b*), we work in a semi-grand-canonical, (N_c, z_p, V, T), ensemble in which the fugacity of the polymers, $z_p = \Lambda_p^{-3} \exp(\beta\mu_p)$, is fixed. μ_p denotes the chemical potential of the reservoir of polymer and $\beta = 1/k_B T$. In addition to the pairwise interactions, we add two, in general different, external fields which couple independently to the colloid and polymer degrees of freedom:

$$V_c^{ext} = \sum_{i=1}^{N_c} v_c^{ext}(\boldsymbol{R}_i), \qquad V_p^{ext} = \sum_{i=1}^{N_p} v_p^{ext}(\boldsymbol{r}_i). \tag{2.3}$$

These potentials create inhomogeneous density profiles $\rho_c(\boldsymbol{r})$ and $\rho_p(\boldsymbol{r})$. The quantity of interest is the Helmholtz free energy, $F(N_c, V, z_p)$. Formally,

$$\exp[-\beta F] = \frac{1}{N_c! \Lambda_c^{3N_c}} \int \mathrm{d}\boldsymbol{R}^{N_c} \exp[-\beta(H_{cc} + \Omega + V_c^{ext})], \tag{2.4}$$

where

$$\exp[-\beta\Omega] \equiv \sum_{N_p=0}^{\infty} \frac{z_p^{N_p}}{N_p!} \int \mathrm{d}\boldsymbol{r}^{N_p} \exp[-\beta(H_{cp} + V_p^{ext})] \tag{2.5}$$

and Λ_i is the thermal de Broglie wavelength of species i $(i = c, p)$. Ω is the grand potential of the ideal polymer coils in the presence of the applied external field V_p^{ext} and the external field that is generated by a fixed configuration of N_c colloids. If one can determine Ω explicitly, one has reduced the difficult problem of treating the

binary system to a much simpler one-component problem: equation (2.4) describes the statistical mechanics of a colloidal system interacting through an effective one-component Hamiltonian $H^{\rm eff} = H_{\rm cc} + \Omega + V_{\rm c}^{\rm ext}$.

For a general binary mixture, Ω consists of an infinite series of terms, representing zero-, one-, two-, ..., many-body contributions (Dijkstra *et al.* 1999*a*). In the particular case of the AO model, each contribution simplifies because $\phi_{\rm pp} = 0$. For a homogeneous (bulk) fluid mixture with $V_{\rm c}^{\rm ext} = V_{\rm p}^{\rm ext} = 0$, $\rho_{\rm c}(\boldsymbol{r})$ and $\rho_{\rm p}(\boldsymbol{r})$ are constant and the series truncates after the two-body term, provided that $q < 2/\sqrt{3} - 1 = 0.1547$ (Gast *et al.* 1983; Dijkstra *et al.* 1999*b*). In this regime of high asymmetry there is no triple overlap of excluded volume regions, even when three colloids are contacting each other. We showed (Brader *et al.* 2001*a*) that similar geometrical considerations apply for the AO mixture in contact with a hard wall defined by

$$v_{\rm c}^{\rm ext}(z) = \begin{cases} \infty, & z < \sigma_{\rm c}/2, \\ 0, & z > \sigma_{\rm c}/2, \end{cases} \qquad v_{\rm p}^{\rm ext}(z) = \begin{cases} \infty & z < \sigma_{\rm p}/2, \\ 0 & z > \sigma_{\rm p}/2, \end{cases} \tag{2.6}$$

where z is the coordinate of the centre of the particle measured normal to the wall. More precisely, we found that for $q < 0.1547$ the effective Hamiltonian for the inhomogeneous system reduces to

$$H^{\rm eff} = H_{\rm cc} + \sum_{i=1}^{N_{\rm c}} v_{\rm c}^{\rm ext}(z_i) + \sum_{i=1}^{N_{\rm c}} \phi_{\rm AO}^{\rm wall}(z_i) + \Omega_0^{\rm bulk} + \Omega_1^{\rm bulk} + \sum_{i<j} \phi_{\rm AO}(R_{ij}), \tag{2.7}$$

where $\phi_{\rm AO}^{\rm wall}$ represents the attractive AO depletion potential between a colloid and the planar hard wall. The depth of this potential is proportional to $z_{\rm p}$ and its range is $\sigma_{\rm p}$. The last three terms of equation (2.7) are those which define Ω for the bulk fluid,

$$-\beta\Omega_0^{\rm bulk} = z_{\rm p} V, \qquad -\beta\Omega_1^{\rm bulk} = -z_{\rm p} N_{\rm c} \pi(\sigma_{\rm c} + \sigma_{\rm p})^3/6 = -z_{\rm p}\eta_{\rm c}(1+q)^3 V,$$

where $\eta_{\rm c} = (\pi/6)\sigma_{\rm c}^3 N_{\rm c}/V$ is the colloid packing fraction. $\phi_{\rm AO}(R)$ is the well-known AO pair potential between two colloids in a sea of ideal polymer. This attractive potential also has range $\sigma_{\rm p}$, is proportional to $z_{\rm p}$, has a similar shape to that of $\phi_{\rm AO}^{\rm wall}$, but is less deep.

It is important to recognize that in the regime $q < 0.1547$ the mapping of the binary mixture to an effective one-component fluid with the Hamiltonian specified by equation (2.7) is *exact* within the AO model. This observation is very significant when we recall that direct simulation of the model binary mixture, which constitutes a very asymmetric system, is prohibited by slow equilibration since huge numbers of polymer are required per colloid particle at state points of interest. It is much easier to perform computer simulations or develop a reliable integral equation theory for the effective Hamiltonian than for the bare binary mixture.

In a bulk fluid the equilibrium structure, i.e. the colloid correlation functions (Dijkstra *et al.* 2000), is determined solely by the effective pair potential,

$$\phi^{\rm eff}(R) = \phi_{\rm cc}(R) + \phi_{\rm AO}(R). \tag{2.8}$$

Moreover since $\Omega_0^{\rm bulk}$ and $\Omega_1^{\rm bulk}$ are linear in $N_{\rm c}$ and V, respectively, they have no effect on the bulk phase equilibria (Dijkstra *et al.* 1999*a*, *b*). These terms do

contribute to the total pressure and total compressibility χ_T of the mixture, making the latter very different from the osmotic compressibility $\chi_{T,\mathrm{eff}}$. More specifically, we find that $\chi_{T,\mathrm{eff}}^{-1}$ makes only a small contribution to the total bulk modulus χ_T^{-1}. It is a term $-k_B T V(\partial z_p/\partial V)_{N_c,N_p}$ determined by the thermodynamics of the reservoir which provides the dominant contribution (Dijkstra *et al.* 2000).

Spontaneously generated inhomogeneities where the density profiles of colloid and polymer are spatially varying in the absence of external fields warrant special attention. Examples are the planar interface between demixed fluid phases, colloidal crystals where the densities vary periodically and the crystal–fluid interface. In such cases H^{eff} reduces to the effective Hamiltonian of the bulk system; there are no additional contributions associated with the inhomogeneity. At first sight this may seem somewhat surprising, as the distribution of polymer in a colloidal crystal, or in the region of the fluid–fluid interface, is clearly very different from that in a bulk fluid and one might imagine that different effective interactions might arise. However, because we work exclusively with a reservoir of polymer, it is the fugacity z_p of this reservoir which controls the interactions in the system. As z_p is constant throughout the inhomogeneous fluid, then so too is the effective interaction between the colloids, regardless of the local polymer density. This serves to reinforce the fact that the species which is integrated out is treated grand-canonically.

We emphasize that for less asymmetric mixtures, with larger size ratios q, the effective Hamiltonian becomes very complex. For $q > 0.25$, the effective pair potential depends on the distance of each colloid centre from the hard wall, not just on their separation R_{ij}, and higher-body potentials are present (Brader *et al.* 2001*a*).

As a final remark on the formal procedure of integrating out the polymer degrees of freedom we note that it is possible, in principle, to recover information about the polymer distribution by performing functional differentiation of the free energy F with respect to $v_p^{\mathrm{ext}}(\boldsymbol{r})$. The polymer density profile $\rho_p(\boldsymbol{r})$ can be expressed in terms of the n-body correlation functions of the colloids as determined from the effective Hamiltonian. In practice, the applicability of this procedure is probably restricted to bulk mixtures with $q < 0.1547$, where one can derive (i) an exact and tractable formula for the free-volume fraction $\alpha(\rho_c; z_p) \equiv \rho_p/\rho_p^r$ of polymer in the fluid mixture and (ii) an approximation for the inhomogeneous polymer density associated with a crystalline array of colloids (Brader *et al.* 2001*a*).

3. Adsorption at a hard wall for size ratio $q = 0.1$

In this section we illustrate the use of the effective Hamiltonian for a mixture with $q = 0.1$. As remarked earlier, the bulk structure is determined solely by $\phi^{\mathrm{eff}}(R)$ the effective pair potential of equation (2.8), and Monte Carlo results for the radial distribution function $g_{cc}(R)$ and structure factor $S_{cc}(k)$ of the colloids at various colloid packing fractions η_c are given by Dijkstra *et al.* (1999*b*). The complete phase diagram of the bulk mixture was also determined by simulation. In the ρ_p^r versus η_c representation there is a very broad, in η_c, fluid–solid coexistence curve which lies well below a metastable fluid–fluid coexistence. Note that the polymer density in the reservoir, ρ_p^r ($\equiv z_p$ for ideal polymer) is equivalent to inverse temperature in simple fluids; each term in the effective Hamiltonian is proportional to z_p. There is also an isostructural (FCC) solid–solid transition which is slightly metastable with respect to the fluid–solid transition (Dijkstra *et al.* 1999*b*). These simulation results provide a

benchmark against which approximate theories can be tested. For example, Percus–Yevick theory, applied with the same $\phi^{\mathrm{eff}}(R)$, yields very accurate colloid radial distribution functions and structure factors while a perturbation theory, based on a hard-sphere reference system, yields a reasonable fluid–solid coexistence curve but the metastable fluid–fluid coexistence is at unphysically high values of η_{c} (Dijkstra *et al.* 1999*b*).

In figure 1 we show Monte Carlo results for the colloid density profile $\rho_{\mathrm{c}}(z)$ in the same mixture adsorbed at a hard wall. These were obtained using the effective Hamiltonian (2.7) and refer to a fixed bulk colloid packing $\eta_{\mathrm{c}} \equiv \pi\sigma_{\mathrm{c}}^3\rho_{\mathrm{c}}(\infty)/6 = 0.4$ and three values of the polymer reservoir packing fraction $\eta_{\mathrm{p}}^{\mathrm{r}} \equiv \pi\sigma_{\mathrm{p}}^3\rho_{\mathrm{p}}^{\mathrm{r}}/6$. In the absence of polymer (figure 1*a*), the system reduces to pure hard spheres at a hard wall and the profile exhibits the usual pronounced oscillations arising from packing effects. On adding a small amount of polymer, $\eta_{\mathrm{p}}^{\mathrm{r}} = 0.05$ (figure 1*b*), the depletion attraction at the wall leads to a much higher contact density $\rho_{\mathrm{c}}(\sigma_{\mathrm{c}}/2)$ than for pure hard spheres at a hard wall. The effect is larger for $\eta_{\mathrm{p}}^{\mathrm{r}} = 0.10$ (figure 1*c*), where the reduced contact density is greater than 20. Plotted alongside the Monte Carlo results are the density profiles obtained from a simple one-component density functional theory (DFT), which treats the hard sphere contribution by the Rosenfeld (1989) fundamental measures theory and the attractive contribution, arising from $\phi_{\mathrm{AO}}(R)$, in mean-field fashion. The overall agreement is quite good although differences do show up on the expanded scale of the insets. A similar trend in the profiles is obtained for $\eta_{\mathrm{c}} = 0.3$ (Brader *et al.* 2001*a*).

While the addition of polymer gives rise to extremely high contact densities the colloid density profiles decay very rapidly to bulk-like values over the small range, $\sigma_{\mathrm{p}} = 0.1\sigma_{\mathrm{c}}$, of the wall depletion potential $\phi_{\mathrm{AO}}^{\mathrm{wall}}$. Crudely speaking, the colloid is behaving as an ideal gas in the deep effective wall potential, with some small enhancement of the local density due to packing effects. The Gibbs adsorption,

$$\Gamma = \sigma_{\mathrm{c}}^2 \int_0^\infty \mathrm{d}z\, (\rho_{\mathrm{c}}(z) - \rho_{\mathrm{c}}(\infty)),$$

does not increase rapidly with increasing $\eta_{\mathrm{p}}^{\mathrm{r}}$ and there is no evidence for any wall-induced local crystallization for the states we have investigated, i.e. up to $\eta_{\mathrm{p}}^{\mathrm{r}} = 0.1$. However, this state point is still substantially removed from the bulk fluid–solid phase boundary. Whether wall induced crystallization sets in at slightly higher polymer packings or whether one must approach very close to the bulk phase boundary in order to observe such a phenomenon remains to be ascertained. One might certainly expect depletion effects to favour the development of crystalline layers prior to bulk crystallization. The main issues are (i) how close to the bulk transition must one be before the first adsorbed layer becomes crystalline and (ii) how do subsequent crystalline layers develop at the hard wall-fluid interface as $\eta_{\mathrm{p}}^{\mathrm{r}}$ is increased (for a fixed η_{c}) towards its value at bulk fluid–solid coexistence? Various scenarios are possible. There could be an infinite sequence of layering transitions culminating in complete wetting of the wall-fluid interface by a nearly close-packed crystal. Alternatively, the interface could remain incompletely wetted by crystal.

We expect similar depletion phenomena for additive binary mixtures of hard spheres near a hard wall, provided the size ratio q is small enough. DFT calculations based on the Rosenfeld (1989) functional for such a binary mixture with $q = 0.1$ yield big sphere (colloid) density profiles which are very similar to those shown here.

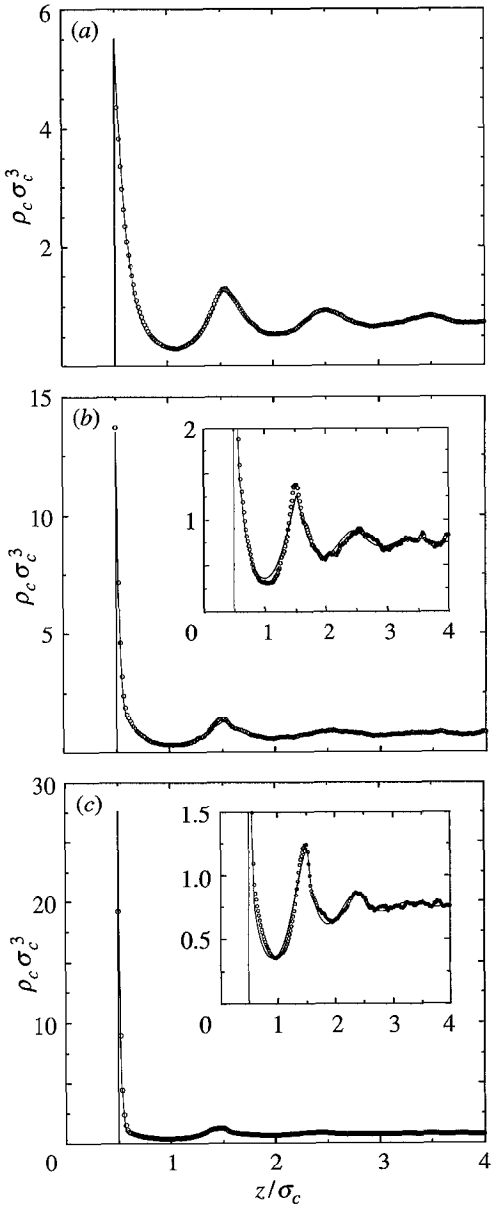

Figure 1. Colloid density profiles near a hard wall: the open circles are the Monte Carlo results while the solid lines denote the one-component DFT results. In each case the bulk colloid packing fraction $\eta_c = 0.4$ and the size ratio $q = 0.1$. The packing fraction of ideal polymer in the reservoir increases from (*a*) $\eta_p^r = 0$ (pure hard spheres) to (*b*) $\eta_p^r = 0.05$ and (*c*) $\eta_p^r = 0.10$. The insets show the results on an expanded vertical scale. Note the rapid increase in contact value $\rho_c(\sigma_c/2)$ as η_p^r is increased.

Once again there is no sign of crystallization at the wall for the state points which were investigated. Detailed comparisons of results for additive hard sphere mixtures with those from the AO model will be presented elsewhere when we shall compare

our findings with those from Poon & Warren (1994), who developed an empirical approach for the calculation of the onset of wall crystallization in additive binary hard sphere mixtures. These authors find hard wall induced crystallization at small sphere packing fractions which are far below the bulk fluid–solid transition. Our results show no evidence of wall induced crystallization at state points where Poon & Warren predict such a transition.

These findings have relevance for real colloidal mixtures in the presence of walls. Several authors have reported evidence for wall induced crystallization well below the bulk fluid–solid phase boundary in mixtures of hard sphere-like colloids at a planar wall. There are also earlier observations of wall induced crystallization in colloid–polymer mixtures (see, for example, Kose & Hachisu 1976; Gast *et al.* 1986). If, as now seems likely, the idealized AO model of a binary colloid–polymer mixture at a planar hard wall predicts that the onset of wall-induced crystallization occurs very close to the bulk transition, this means that factors other than depletion must be important in the experiments. These may include polydispersity, which could play a different role in wall crystallization from that in bulk crystallization, and the fact that the actual wall–colloid potential could be different from that of a hard wall. Any residual attractive dispersion forces between the substrate and the colloid could favour the onset of wall-induced crystallization. The theoretical framework which we have developed allows us to obtain reliable results for the well-defined AO model, which although simple, does incorporate the key features of depletion-induced colloid–colloid and wall–colloid attraction. As such it provides a valuable means of studying the effects of depletion on interfacial properties. The drawback is that the procedure is, for most practical purposes, restricted to $q < 0.1547$.

4. Density functional theory for the binary AO model

As emphasized in § 2, formally integrating out the polymer degrees of freedom yields very complicated effective Hamiltonians for the colloids when $q > 0.1547$. In order to tackle less asymmetric mixtures, an alternative strategy is required. Since direct simulation of the binary system is not practicable because of the large numbers of polymer coils required, we have designed a DFT specifically for the binary AO mixture (Schmidt *et al.* 2000). Here we describe the functional and report some results of its application to adsorption at a hard wall and to the properties of the free fluid–fluid interface.

(*a*) *Description of the density functional*

The procedure for constructing the DFT is based on the successful fundamental measures theory developed by Rosenfeld (1989) for additive hard sphere mixtures and the excess, over ideal, Helmholtz free energy functional is given by an equivalent form:

$$\beta F_{\mathrm{exc}}[\rho_{\mathrm{c}}(\boldsymbol{r}), \rho_{\mathrm{p}}(\boldsymbol{r})] = \int \mathrm{d}^3x\, \Phi(\{n_\nu^{\mathrm{c}}(x)\}, \{n_\lambda^{\mathrm{p}}(x)\}). \tag{4.1}$$

The weighted densities are

$$n_\nu^i(\boldsymbol{x}) = \int \mathrm{d}^3r\, \rho_i(\boldsymbol{r})\omega_\nu^i(\boldsymbol{x}-\boldsymbol{r}),$$

where the weight functions are $\omega_3^i(\boldsymbol{r}) = \theta(R^i - r)$, $\omega_2^i(\boldsymbol{r}) = \delta(R^i - r)$, $\boldsymbol{w}_{v2}^i(\boldsymbol{r}) = \omega_2^i(\boldsymbol{r})\boldsymbol{r}/r$, and where $r = |\boldsymbol{r}|$, $\theta(r)$ is the step function and $\delta(r)$ is the Dirac distribution. Further weights are $\omega_1^i(\boldsymbol{r}) = \omega_2^i(\boldsymbol{r})/(4\pi R^i)$, $\boldsymbol{w}_{v1}^i(\boldsymbol{r}) = \boldsymbol{w}_{v2}^i(\boldsymbol{r})/(4\pi R^i)$, $\omega_0^i(\boldsymbol{r}) = \omega_1^i(\boldsymbol{r})/R^i$. There are four scalar and two vector ($\boldsymbol{w}_{v1}$ and $\boldsymbol{w}_{v2}$) weight functions. R^i denotes the radius of species i, with $i = \mathrm{c}, \mathrm{p}$, so that $R^{\mathrm{c}} = \sigma_{\mathrm{c}}/2$ and $R^{\mathrm{p}} = \sigma_{\mathrm{p}}/2$. In order to obtain the free energy density Φ appropriate to the AO model, Schmidt *et al.* (2000) considered the zero-dimensional limit which corresponds to a cavity that can hold at most one colloid but can hold an arbitrary number of ideal polymer coils if no colloid is present. We found

$$\Phi = n_0^i\varphi^i(n_3^{\mathrm{c}}, n_3^{\mathrm{p}}) + (n_1^i n_2^j - \boldsymbol{n}_{v1}^i \cdot \boldsymbol{n}_{v2}^j)\varphi^{ij}(n_3^{\mathrm{c}}, n_3^{\mathrm{p}}) + \frac{1}{8\pi}(n_1^i n_2^j n_2^k/3 - n_2^i \boldsymbol{n}_{v2}^j \cdot \boldsymbol{n}_{v2}^k)\varphi^{ijk}(n_3^{\mathrm{c}}, n_3^{\mathrm{p}}), \quad (4.2)$$

where the Einstein summation convention is used, and

$$\varphi^{i\ldots k}(\eta_{\mathrm{c}}, \eta_{\mathrm{p}}) \equiv \frac{\partial^m \beta F_{0\mathrm{d}}(\eta_{\mathrm{c}}, \eta_{\mathrm{p}})}{\partial\eta_i \ldots \partial\eta_k}.$$

Here

$$\beta F_{0\mathrm{d}}(\eta_{\mathrm{c}}, \eta_{\mathrm{p}}) = (1 - \eta_{\mathrm{c}} - \eta_{\mathrm{p}})\ln(1 - \eta_{\mathrm{c}}) + \eta_{\mathrm{c}}$$

is the excess free energy appropriate to this particular cavity, and η_{c} and η_{p} are the packing fractions of the two species. In the original paper, Schmidt *et al.* included a tensor weight function; this is omitted here. The functional can also be regarded as a linearization, in the polymer density, of the original Rosenfeld functional.

For a homogeneous (bulk) fluid mixture our functional yields the excess Helmholtz free-energy density $\beta F_{\mathrm{exc}}(\rho_{\mathrm{c}}, \rho_{\mathrm{p}})/V = \beta f_{\mathrm{hs}}(\rho_{\mathrm{c}}) - \rho_{\mathrm{p}} \ln \alpha(\rho_{\mathrm{c}})$, where $f_{\mathrm{hs}}(\rho_{\mathrm{c}})$ is the excess free-energy density of pure hard spheres in the scaled-particle (Percus–Yevick compressibility) approximation and $\alpha = (1 - \eta_{\mathrm{c}})\exp(-A\gamma - B\gamma^2 - C\gamma^3)$, with $\gamma = \eta_{\mathrm{c}}/(1 - \eta_{\mathrm{c}})$, $A = q^3 + 3q^2 + 3q$, $B = 3q^3 + 9q^2/2$, and $C = 3q^3$. This result is *identical* to that of the free-volume theory of Lekkerkerker *et al.* (1992) for the AO model, which is known to yield stable colloidal gas–liquid coexistence for size ratios $q \geqslant 0.32$. For smaller q this fluid–fluid transition becomes metastable with respect to a broad, in η_{c}, fluid–solid transition.

The bulk pair direct correlation functions $c_{ij}^{(2)}$ obtained by differentiating $F_{\mathrm{exc}}[\rho_{\mathrm{c}}, \rho_{\mathrm{p}}]$ are given analytically. The Ornstein–Zernike relations then provide the bulk partial structure factors $S_{ij}(k)$. As a consequence of linearization in the polymer density, $c_{\mathrm{pp}}^{(2)} = 0$, as in Percus–Yevick approximation for this model. The other two functions $c_{\mathrm{cc}}^{(2)}$ and $c_{\mathrm{cp}}^{(2)}$ are not the same as those from Percus–Yevick theory. Nevertheless, the resulting analytical $S_{ij}(k)$ are of a similar quality to those obtained from numerical solutions of the binary mixture Percus–Yevick integral equations (Schmidt *et al.* 2000). An important advantage of the present DFT over integral equation theories is that the structure factors and radial distribution functions, obtained from the Ornstein–Zernike route, are consistent with the bulk free energy, i.e. thermodynamic and structural routes to the fluid–fluid spinodal and critical point are equivalent. This property is particularly advantageous when one investigates interfaces at or near two-phase coexistence.

The functional treats colloid and polymer on equal footing. For inhomogeneous situations the colloid and polymer density profiles are obtained by minimizing the

grand potential functional,

$$\Omega[\rho_c, \rho_p] = F_{id}[\rho_c, \rho_p] + F_{exc}[\rho_c, \rho_p] + \sum_{i=c,p} \int d^3r \, (V_i^{ext}(\boldsymbol{r}) - \mu_i)\rho_i(r), \qquad (4.3)$$

where $F_{id}[\rho_c, \rho_p]$ is the ideal gas free energy functional and μ_i is the chemical potential of species i. Solving the resulting Euler–Lagrange equations is somewhat simpler than for a general binary mixture since $\rho_p(\boldsymbol{r})$ is an explicit functional of $\rho_c(\boldsymbol{r})$ and $V_p^{ext}(\boldsymbol{r})$; only $\rho_c(\boldsymbol{r})$ needs to be determined by numerical minimization.

(*b*) *Wetting and layering transitions at a hard wall*

Since our DFT incorporates bulk fluid–fluid phase separation it can be used to investigate fluid wetting phenomena at solid substrates. We choose to consider a planar hard wall defined by equation (2.6). For such a model we expect entropic depletion effects to favour the adsorption of colloid-rich phase at the wall so we might expect to observe complete wetting by this phase at the hard wall–colloid-poor interface.

In order to test the DFT we first calculated density profiles for $q = 0.1$, the mixture considered in § 3, for which Monte Carlo results are available for the colloid profile; recall that the mapping to the effective Hamiltonian (2.7) is exact in this case. Our functional provides a very good description of the Monte Carlo results; the agreement is of similar quality to that between the simulation and one-component DFT results shown in figure 1. Explicit comparisons of theory and simulation results will be presented elsewhere, but we confirmed that the functional does account for the depletion attraction between the hard wall and the colloids.

We focus now on larger size ratios where a stable fluid–fluid transition occurs. Figure 2 shows the bulk phase diagram obtained from the present theory for a size ratio $q = 0.6$ for which the fluid–fluid demixing transition has a critical point at $\eta_{p,crit}^r \sim 0.495$. It should be emphasized that the fluid–fluid and solid–fluid phase boundaries presented here are those of the original free-volume theory of Lekkerkerker *et al.* (1992). A full investigation of the freezing properties of the present functional is outside the scope of the current study which is restricted to fluid states. Also shown in figure 2 is the Fisher–Widom (FW) line which divides the phase diagram into regions where the asymptotic decay of bulk pairwise correlations, $g_{ij}(r)$, is either monotonic or exponentially damped oscillatory (Evans *et al.* 1994). The FW line was determined by calculating the poles of the partial structure factors $S_{ij}(k)$. Note that in a binary mixture the three $g_{ij}(r)$ change simultaneously their asymptotic decay as the FW line is crossed.

In determining the adsorption characteristics, we choose to fix η_p^r and approach the bulk phase boundary from the colloid-poor side. This is analogous to performing a gas adsorption *isotherm* measurement for a simple fluid. Recall that η_p^r plays a role equivalent to inverse temperature. Depending on the value of η_p^r chosen, the adsorption behaviour changes dramatically. We consider size ratio $q = 0.6$ and describe some of the phenomena encountered. We first choose a path just above the critical point, with $\eta_p^r = 0.55$; see path I in figure 2. On approaching the phase boundary we find that the wall is completely wet by the colloid-rich phase. Figure 3 shows the colloid profiles signalling the growth of a thick layer of colloidal liquid against the wall. The corresponding polymer profiles are shown in the inset and indicate how

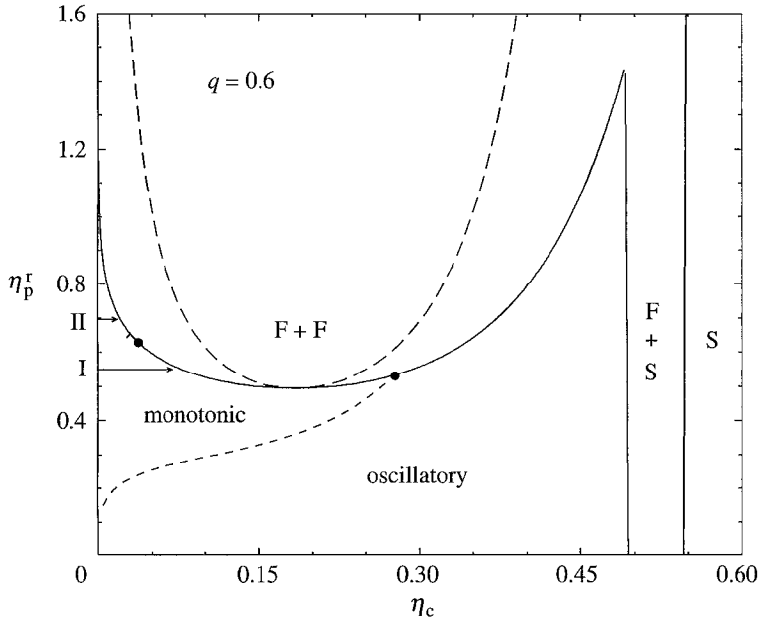

Figure 2. The bulk phase diagram calculated from free volume theory for $q = 0.6$. η_c is the packing fraction of the colloid and η_p^r that of polymer in the reservoir. F denotes fluid and S solid. The long-dashed line shows the fluid–fluid spinodal and the short-dashed line shows the Fisher–Widom line obtained from DFT. The latter intersects the binodal at $\eta_{p,FW}^r = 0.53$. Horizontal arrows indicate the paths I and II by which the phase boundary is approached for the adsorption studies. The point on the binodal at $\eta_{p,w}^r \approx 0.63$ indicates the location of the wetting transition.

polymer becomes more depleted as the colloid-rich layer grows. Strictly speaking, *macroscopically* thick wetting films can only occur on the monotonic side of the FW line, i.e. for $\eta_p^r < \eta_{p,FW}^r$, the point of intersection of the FW line and the binodal, since oscillatory binding potentials will stabilize very thick but finite films which would otherwise be infinite (Henderson 1994). For $\eta_p^r = 0.55$ (path I) we can easily obtain films of thickness 20 or $30\sigma_c$ and in the flat portion of the profiles the densities of colloid and polymer are equal to their values in the coexisting colloid-rich phase. At large values of η_p^r (> 0.75), we find that the wall is incompletely wetted by colloid; the layer thickness increases continuously remaining finite at the phase boundary. At lower values ($0.6 < \eta_p^r < 0.75$), we find a single, first order layering transition. This is illustrated in figure 4, where the colloid profiles are plotted for $\eta_p^r = 0.7$, following path II in figure 2, along with the Gibbs adsorption Γ. At the transition the densities $\rho_c(z)$ in the first (contact) layer and in the second layer increase substantially and Γ jumps discontinuously. Γ remains finite at bulk coexistence, i.e. there is still partial wetting. The layering transition line ends in a critical point at $\eta_p^r \approx 0.62$; the jump in the adsorption disappears for smaller η_p^r. It would appear that the layering represents a quasi-two-dimensional gas–liquid condensation transition. The layering transition line is quite separate from the prewetting line which emerges tangentially from the bulk coexistence curve at $\eta_{p,w}^r \approx 0.63$ (the wetting transition 'temperature') and ends in the prewetting critical point at $\eta_p^r \approx 0.60$. This pattern of surface transitions appears to be quite different from what is usually found for

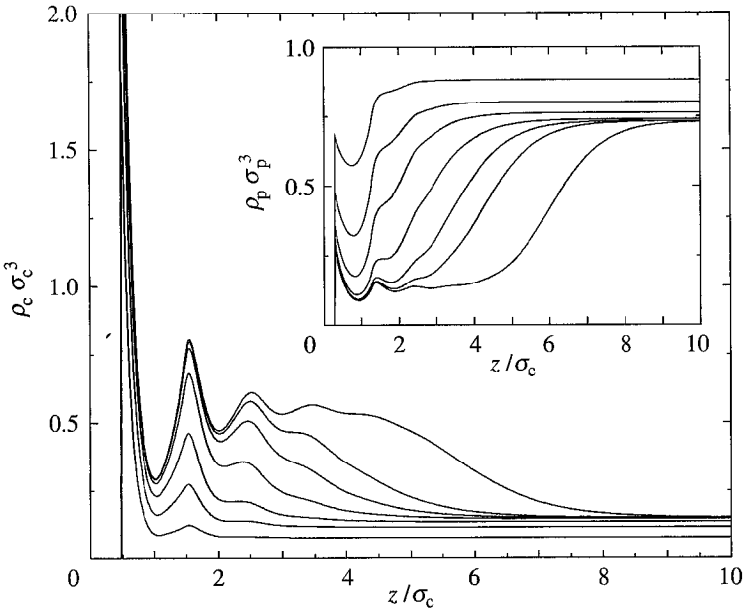

Figure 3. Colloid density profiles for $q = 0.6$ showing the complete wetting of a hard wall by the colloid-rich phase at $\eta_p^r = 0.55$ as the bulk phase boundary is approached along path I in figure 2. Bulk colloid fractions are $\eta_c = 0.04$, 0.06, 0.07, 0.076, 0.0775, 0.0778 and 0.0779 (from bottom to top). The inset shows the polymer profiles for the same η_c (from top to bottom).

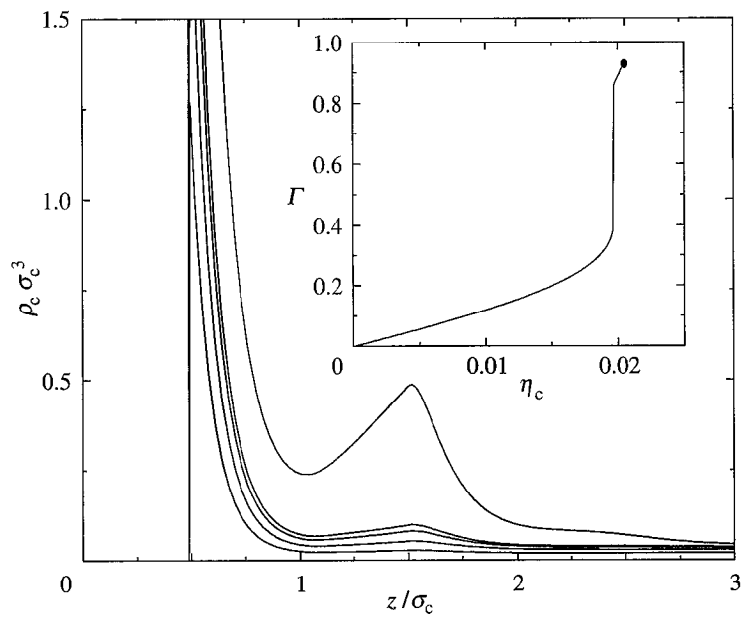

Figure 4. Colloid density profiles for $q = 0.6$ showing the layering transition at $\eta_p^r = 0.7$ corresponding to path II in figure 2. Bulk colloid fractions are $\eta_c = 0.010$, 0.015, 0.018, 0.019 and 0.020 (from bottom to top); the transition occurs between 0.019 and 0.020. The inset shows the corresponding Gibbs adsorption Γ; this remains finite at bulk coexistence $\eta_c = 0.0203$.

simple fluids adsorbed at strongly attractive substrates where, for temperatures not too far from the triple point, complete wetting often proceeds via a sequence (possibly infinite) of layering transitions (see, for example, Ball & Evans 1988). Here we have a *single* transition, distinct from prewetting, which occurs well away from the triple point; the latter is at $\eta_{\mathrm{p}}^{\mathrm{r}} \approx 1.43$ in the free-volume theory. It is very likely that the occurrence of the layering transition reflects the underlying difference between a one-component fluid, described by a simple pairwise fluid–fluid potential and a simple one-body wall-fluid potential representing interactions with a substrate, and the present binary AO mixture. As we have seen in § 2, the effective one-component Hamiltonian involves pairwise potentials which depend on the distance of the colloids from the wall as well as complex higher-body interactions for these (large) size ratios.

Although we have yet to determine how the pattern of surface transitions depends on the size ratio q, and there might well be surprises in store, we believe our present predictions of entropically driven wetting and layering transitions might encourage experimental investigations of adsorption in colloid–polymer mixtures. Real space techniques, such as confocal microscopy, may provide a useful tool for observing wetting in colloidal suspensions. Measurements of the contact angle θ formed at the contact line between the colloid-rich–colloid-poor (liquid–gas) interface and a suitable substrate modelling a hard wall could also be revealing. We are predicting that the colloidal liquid phase should incompletely wet the substrate ($\theta > 0$) for $\eta_{\mathrm{p}}^{\mathrm{r}} > \eta_{\mathrm{p,w}}^{\mathrm{r}}$, the wetting transition value, and wet completely ($\theta = 0$) for $\eta_{\mathrm{p}}^{\mathrm{r}} < \eta_{\mathrm{p,w}}^{\mathrm{r}}$.

(*c*) *The structure and tension of the fluid–fluid interface*

We have also calculated the properties of the free liquid–gas interface between demixed fluid phases using our new DFT approach. Detailed results are given in Brader *et al.* (2001*b*); here we merely state the main findings. For $q = 0.6$ and 1.0, the two cases investigated in most detail, we find that the width of the interface is about one colloid diameter for states near the bulk triple point. This width is similar to estimates inferred from recent ellipsometric measurement on a real colloid–polymer mixture (de Hoog *et al.* 1999). The surface tension we calculate agrees reasonably well with data obtained from spinning-drop and breaking-thread measurements for mixtures of a silica colloid, coated with 1-octadecanol, and polydimethylsiloxane (PDMS) in cyclohexane at $T = 293\,\mathrm{K}$ (de Hoog & Lekkerkerker 1999). The size ratio for this mixture is approximately 1.0. In order to compare our DFT results with experiment we choose $\sigma_{\mathrm{c}} = 26\,\mathrm{nm}$, the mean diameter of the particles investigated in the experiment; there are no other adjustable parameters in the theory. The measured and calculated tensions are 3–4 $\mu\mathrm{N\,m^{-1}}$, values which are about 1000 times smaller than tensions of simple fluids. Such small tensions result from the fact that colloids are much larger than atoms or simple molecules; the tension scales roughly as $k_{\mathrm{B}}T\eta_{\mathrm{p}}^{\mathrm{r}}/\sigma_{\mathrm{c}}^2$ for states well removed from the critical point (Brader & Evans 2000). The most striking results which emerge from the DFT are those for the form of the density profiles $\rho_{\mathrm{c}}(z)$ and $\rho_{\mathrm{p}}(z)$. We find that when $\eta_{\mathrm{p}}^{\mathrm{r}}$ is sufficiently high, i.e. well removed from the critical point, both $\rho_{\mathrm{c}}(z)$ and $\rho_{\mathrm{p}}(z)$ exhibit oscillations on the colloid-rich (liquid) side of the free interface. The period, which is about σ_{c}, and the decay length of the oscillations are identical for both species, in keeping with general arguments concerning asymptotic decay of correlation functions in mixtures (Evans *et al.* 1994). For states with $\eta_{\mathrm{p}}^{\mathrm{r}} < \eta_{\mathrm{p,FW}}$ (see figure 2), both $\rho_{\mathrm{c}}(z)$ and

$\rho_{\rm p}(z)$ decay monotonically into the bulk liquid. Although similar oscillations with a period of about one atomic diameter, are seen in DFT studies of the free liquid–gas interface for simple fluids near their triple points (Evans *et al.* 1993) here the amplitude of the oscillations in the colloid profile appears to be larger. Of course DFT treatments are mean-field-like in that they ignore the effects of capillary-wave fluctuations of the interface. We are presently investigating whether including these fluctuation effects will completely erode the oscillations or whether some oscillatory structure will remain in the 'dressed' colloid profile. From an experimental viewpoint it should be more favourable to investigate such structuring in colloidal fluids, where the period is of colloidal size, than in simple, atomic fluids.

5. Concluding remarks

Two different but complementary strategies for tackling the statistical mechanics of the AO model have been adopted. In the first we performed a formal integrating out of the polymer degrees of freedom to obtain an effective Hamiltonian for the colloids. Such a strategy is especially valuable for size ratio $q < 0.1547$, where the resultant effective Hamiltonian is exact and is sufficiently simple, even for inhomogeneous mixtures, to be investigated using computer simulation methods. The mapping makes tractable a difficult binary mixture problem which would not be tractable by direct simulation methods. This strategy has also proved valuable for determining the bulk phase behaviour of highly asymmetric binary mixtures of additive hard spheres (Dijkstra *et al.* 1999*a*). In this case the mapping to an effective one-component system of big spheres involves an infinite sum of terms for *any* value of q. However, if one truncates the series after the two-body (depletion potential) contribution, simulation results for the effective Hamiltonian capture accurately all the key features of the bulk phase equilibria as determined by direct simulation of the binary hard-sphere mixture—at least for size ratios up to $q = 0.2$ (Dijkstra *et al.* 1999*a*). How far in q one can trust an *approximate* effective Hamiltonian for studies of adsorption remains to be ascertained.

In the second strategy we did not perform any integrating out of the polymer degrees of freedom, rather we developed an approximate DFT for the binary AO mixture. Since there is no explicit integrating out, the DFT is applicable for all size ratios. This permits us to investigate mixtures for which stable fluid–fluid phase separation occurs, and allows us to tackle wetting and related adsorption phenomena as well as the free fluid–fluid interface. The same DFT could, in principle, be used to tackle bulk fluid–solid (freezing) transitions and the corresponding solid–fluid interface. It could also be used to investigate wall-induced crystallization, although this is a very demanding problem in DFT or in simulation. Confined mixtures constitute another class of problem which is well suited to investigation by DFT and we have observed capillary condensation phenomena when the mixture is confined between two parallel planar hard walls. Since the walls prefer the colloid-rich (liquid) phase, condensation occurs on the low $\eta_{\rm c}$ side of the coexistence curve (J. M. Brader 2000, unpublished work). We should emphasize that unlike DFT treatments of interfacial phenomena in simple fluids, where there is an explicit attractive fluid–fluid potential which is usually treated in a perturbative (mean-field) fashion (see, for example, Evans 1992), here the effective attractive interactions emerge from the theory and they are not treated perturbatively.

In summary we have shown that interfacial properties of the simplest model colloid–polymer mixture can be extremely rich. That such a diversity of phenomena should arise in a system where the bare interactions are either hard or ideal is remarkable and points to the importance of entropic depletion forces in determining surface as well as bulk phase behaviour.

We thank E. H. A. de Hoog, A. Gonzalez, H. N. W. Lekkerkerker, A. A. Louis, R. P. Sear, M. M. Telo da Gama and P. B. Warren for helpful discussions. R. van Roij provided valuable insight into matters concerned with integrating out degrees of freedom and understanding the status of the resulting effective Hamiltonians. This research was supported by the British–German ARC Programme (Project 104b) and by DFG Lo 418/5.

References

Asakura, S. & Oosawa, F. 1954 *J. Chem. Phys.* **22**, 1255.

Ball, P. C. & Evans, R. 1988 *J. Chem. Phys.* **89**, 4412.

Brader, J. M. & Evans, R. 2000 *Europhys. Lett.* **49**, 678.

Brader, J. M., Dijkstra, M. & Evans, R. 2001*a* *Phys. Rev.* E. (In the press.)

Brader, J. M., Evans, R., Schmidt, M. & Löwen, H. 2001*b* (Submitted.)

de Hoog, E. H. A. & Lekkerkerker, H. N. W. 1999 *J. Phys. Chem.* B **103**, 5274.

de Hoog, E. H. A., Lekkerkerker, H. N. W., Schulz, J. & Findenegg, G. H. 1999 *J. Phys. Chem.* B **103**, 10657.

Dijkstra, M., van Roij, R. & Evans, R. 1999*a* *Phys. Rev.* E **59**, 5744.

Dijkstra, M., Brader, J. M. & Evans, R. 1999*b* *J. Phys. Cond. Matt.* **11**, 10079.

Dijkstra, M., van Roij, R. & Evans, R. 2000 *J. Chem. Phys.* **113**, 4799.

Evans, R. 1992 In *Fundamentals of inhomogeneous fluids* (ed. D. Henderson), ch. 3, p. 85. Dekker.

Evans, R., Henderson, J. R., Hoyle, D. C., Parry, A. O. & Sabeur, Z. A. 1993 *Molec. Phys.* **80**, 755.

Evans, R., Leote de Carvalho, R. J. F., Henderson, J. R. & Hoyle, D. C. 1994 *J. Chem. Phys.* **100**, 591.

Gast, A. P., Hall, C. K. & Russel, W. B. 1983 *J. Colloid Interface Sci.* **96**, 251.

Gast, A. P., Russel, W. B. & Hall, C. K. 1986 *J. Colloid Interface Sci.* **109**, 161.

Henderson, J. R. 1994 *Phys. Rev.* E **50**, 4836.

Ilett, S. M., Orrock, A., Poon, W. C. K. & Pusey, P. N. 1995 *Phys. Rev.* E **51**, 1344.

Kose, A. & Hachisu, S. 1976 *J. Colloid Interface Sci.* **55**, 487.

Lekkerkerker, H. N. W., Poon, W. C. K., Pusey, P. N., Stroobants, A. & Warren, P. B. 1992 *Europhys. Lett.* **20**, 559.

Poon, W. C. K. & Warren, P. B. 1994 *Europhys. Lett.* **28**, 513.

Rosenfeld, Y. 1989 *Phys. Rev. Lett.* **63**, 980.

Schmidt, M., Löwen, H., Brader, J. M. & Evans, R. 2000 *Phys. Rev. Lett.* **85**, 1934.

Vrij, A. 1976 *Pure. Appl. Chem.* **48**, 471.